HYDRODYNAMICS AND ELECTROCHEMISTRY OF SILICA SCALING

P. Kokhanenko [1], S. Masuri [1], M. Jermy [1], M. Sellier [1] and K. Brown [2]

[1] University of Canterbury with full contact address and country name

[2] Second Affiliation with full contact address and country name

pavlo.kokhanenko@pg.canterbuty.ac.nz

Keywords: *silica scale, colloidal silica, hydrodynamic effects, surface chemistry.*

ABSTRACT

Geothermal brine is saturated with silica (with respect to quartz) in the reservoir, can become supersaturated (with respect to amorphous silica) when steam is extracted or the brine cooled in a powerplant. The excess silica precipitates either as colloidal particles which may subsequently deposit on surfaces (pipe or rock fissure walls), or a vitreous film on those surfaces formed from monomeric silica. This scale may obstruct pipes and reinjection wells and limit the efficacy of heat exchangers. The transport of colloidal silica to the wall is influenced by temperature, particle size, flow velocity and also by pH, ionic strength and the species present at the wall, which affect the magnitude of the repulsive electrical double-layer force and the attractive, short-range London forces. The theory of colloid growth and transport is reviewed and timescales for key steps is calculated, for conditions representative of NZ geothermal plant. Data from a recirculating flow rig is presented, showing the effect of temperature, particle size, flow structure and surface morphology on the rate of deposition in mild steel pipes. Colloidal silica tends to deposit first in isolated clusters, whose size and location is influenced by chemical and local hydrodynamic conditions.

1. INTRODUCTION

Silica scaling occurs where geothermal water, initially in equilibrium with quartz, becomes supersaturated with respect to amorphous silica by loss of steam or heat.

The scaling may occur as a chemisorption of single silicic acid molecules directly from solution to a wall or by the formation of colloidal silica particles in a solution, followed by their transport and attachment to the wall. The second mechanism, of colloidal deposition, results in a much greater scaling rate. It is not sufficiently understood because of the conjunction of chemical and hydrodynamic phenomena.

1.1 CHEMISTRY OF COLLOIDAL SILICA

The properties of both dissolved and colloidal silica were studied extensively [1] as the latter has wide industrial application. Based on his own [2] and preceding experimental results [3] Fleming showed that colloidal silica particles form in four steps. First, formation of silica polymers takes place. Individual silicic acid molecules bond together forming polymers – nuclei.

For these nuclei to become centres of subsequent silica condensation they need to grow over a critical radius. This second step is called Ostwald ripening. The time required for its completion was found [2, 3] to be an exponential function of the silica oversaturation ratio and pH. The rate of formation of colloidal particles depends on the silica saturation index $\left(SSI = \frac{Actual\ \ Silica\ \ Concentration}{Saturation\ \ Silica\ \ Concentration} \right)$.

Based on empirical results by Weres at al. [3] nucleation times for the brine conditions after steam separation are, for a particular case:

- without acid dosing: pH=7.5, T=150°C, SSI_0=2.5 - $\tau_{nuc} = 5 - 10\,\text{min}$
- with acid dosing: pH=5.7, T=150°C, SSI_0=2.5 - $\tau_{nuc} \geq 10000\,\text{min}$

Next, decelerating growth of these particles continues by the chemisorption of the silicic acid molecules from the solution onto the surface of the particle. The rate of this polymerization reaction is directly proportional to the surface concentration of ionized hydroxyl groups, SiO^-:

$$\frac{-dC}{dt} = kA_s[SiO^-](C - C_X)$$

here A_s is the surface area of the silica present, and C is the dissolved silica concentration in mg/kg:

$C_X = C_e \frac{\Gamma_{sat}}{\Gamma_e}$ - pseudoequilibrium silica concentration;

C_e – silica solubility; Γ_{sat}, Γ_e - max and equilibrium surface concentration of chemisorbed silicic acid, $-Si(OH_3)$;

$k = A_0 \exp\frac{-E}{RT}$ – rate constant,

with the pre-exponential factor A_0 and activation energy E determined by Fleming [2]

$\ln A_0 = 22.1 \pm 1.5$, $E = 13.1 \pm 0.9 kcal/mole$

so $\ln k = 22.1 - \frac{13100}{RT} \pm 2$.

Thus it increases with pH and temperature, and also with salt concentration (not shown above, see [2]). The concentration of dissolved silica decreases most significantly over this step.

Using Fleming's experimental results, characteristic times of particle growth for the brine conditions after steam separation can be estimated as:

- without acid dosing: pH=7.5, T=150°C, SSI_0=2.5 - $\tau_{chsorb} = 100 - 200\,\text{min}$
- with acid dosing: pH=5.7, T=150°C, SSI_0=2.5 - $\tau_{chsorb} \approx 3000\,\text{min}$

Once the concentration of ionized hydroxyl groups drops to the equilibrium level, determined by amorphous silica solubility, the overall particle growth rate becomes limited

by the kinetics of surface rearrangement. Neighboring chemisorbed silicic acid molecules $-Si(OH)_3$ form interconnecting bonds and thus incorporate into solid silica $\equiv SiOH$. The rate of this final step of colloidal AS silica formation varies with temperature per the Arrhenius law and with pH and ionic strength only through the silica solubility:

$$\frac{-dC}{dt} = K_{sr}(C - C_e)^3$$

where $K_{sr} = k_{sr} A_s \Gamma_e^2 C_e^{-2}$ - rate constant of the surface rearrangement (*sr*) reaction;

and $k_{sr}\Gamma_e^2 = A_{sr} \exp\frac{-E_{sr}}{RT}$

$$\ln A_{sr} = 13.7 \pm 2.7$$
$$E_{sr} = 13.5 \pm 1.8 kcal/mole$$
$$\ln k_{sr}\Gamma_e^2 = 13.7 - \frac{13500}{RT} \pm 4.0$$

Evidently, characteristics of the resultant silica sol are strongly dependent on the initial level of silica oversaturation, pH and the presence of other elements dissolved in the solution.

As with any colloidal system, silica sol can be characterized by the level of aggregative stability, or stability ratio $W = \frac{Number\ of\ collisions\ between\ particles}{Number\ of\ collisions\ resulting\ in\ coagulation}$ [4]. Suspended in the solution, particles undergo continuous mutual collisions due to their Brownian motion. Without any constraint in place those lead to a rapid coagulation, limited only by the rate particle diffusion towards one another – a few particles stick together after collision, form growing aggregates and eventually separate from the solution. The time required for the number of particles to be reduced to half of the initial value equals [4]:

$$t_{1/2} = 1/8\pi Dan_0$$

here *a* is a particle radius, n_0 - bulk particle concentration cm^{-3} and - $D = kT/6\pi\eta a$ is a particle diffusion coefficient [5], η-fluid viscosity. The rate of rapid coagulation does not depend on particle size and in water at 25°C $t_{1/2} \approx \left(2\times10^{11}/n_0\right)$ seconds. Synthetic silica sols used in this work have n_0 values of about 10^{11} cm^{-3} and so have a rapid coagulation in seconds range. $t_{1/2}$ also depends on ionic strength (see below).

However colloidal silica particles are usually charged and surrounded by repulsive double layer potential which serves as a barrier making most collisions reflective. The effectiveness of this electrostatic colloidal stabilization depends on the ratio between the potential height ($V=V_{max}$) and a particle kinetic energy due to the Brownian motion (kT):

$W = \int_2^\infty \exp\left(\frac{V}{kT}\right)\frac{ds}{s^2}$ - here $s=r/a$ is a non-dimensional distance between particles.

Typically for colloidal particles existence of this barrier reduces the aggregation rate by factor of 10^3 if compared to uncharged particles [4].

1.2 SILICA TRANSPORT

Scale formation naturally implies transport of the silica to the surface. The following paragraphs discuss how the rate of this transport depends on the hydrodynamics of suspending flow and size of the depositing silica particles.

For the geothermal plant operation scaling in two flow scenarios is of interest. In the reinjection lines highly turbulent pipe flow with a well defined near-wall velocity structure forms. Whereas, inside irregular rock fissures and pores it is more complex with no stable developed characteristics. Flow tends to be at low Reynolds numbers in rocks.

Generally, two conceptually different mechanisms are responsible for the mass transfer – molecular (or Brownian for particles) and convective diffusion [6]. The relative importance of these mechanisms is determined by the value of the dimensionless Schmidt number: $Sc = \frac{\nu}{D}$, where ν - fluid viscosity, D - diffusion coefficient. The molecular diffusion coefficient for silicic acid in water at 25°C was determined experimentally by Applin [7] to be 2.2 $*10^{-9}$ m^2sec^{-1}. The Brownian diffusion coefficient for 100 nm diameter colloidal particle in same conditions is $4.3*10^{-12}$ m^2sec^{-1} and it is inversely proportional to the particle size [5]. Due to the high viscosity of water (10^{-6} m^2sec^{-1}) convective diffusion prevails even for very low flow velocities, under the conditions relevant to geothermal plant. Thus it is only very close to the wall boundary, where the flow velocity tends to 0, that molecular (or Brownian) diffusion becomes important. This region is called the diffusion boundary layer and it is the main resistance to mass transfer. The height of this layer depends on the structure of the hydrodynamic boundary layer. It was shown to be as small as 1/10 of the viscous sublayer height [6]. Thus, noticeable changes in silica concentration can take place only inside this layer, while outside it turbulent/convective diffusion provides uniform concentration distribution. Overall the rate of the diffusion mass transfer increases with the corresponding diffusion coefficient and local concentration gradient, which is inversely proportional to the height of the local viscous boundary sublayer.

Even though colloidal particles have much lower diffusion rate than silicic acid molecules, it was shown [8, 9] that they are responsible for higher scaling rates. Experimental results from the present work will be shown to agree with this.

Dunstall and Brown [9] experimentally studied scaling on the steel cylinder subjected to the cross flow of the silica aquasol. They measured the deposition rate to increase with the particle size and to be a function of location across cylinder circumference. Thus, he suggested inertial effects to increase colloidal silica transport rate.

The mass transport though the boundary layer of particles suspended in flowing media can be facilitated by inertial effects. The projections caused by flow streamline curvature and turbulence dispersion [10], turbophoresis [11, 12] and Saffman lift [13] were determined by Epstein [14]

as the most important. In his review paper [14] on deposition from the parallel suspending flows he gives a semi-empirical classification of the dominant transport mechanisms for increasing non-dimensional particle relaxation time $\tau_p^+ = \frac{\rho_p d_p^2}{18\eta} \cdot \frac{(\upsilon^*)^2}{\nu}$ (so does its diameter d_p^2) – diffusion prevails for $\tau_p^+ < 10^{-1}$, inertia - at $\tau_p^+ < 10$ and impaction for even bigger particles. Epstein mentioned the significance of the Saffman lift, but did not include it in the above classification.

Sinclair [15] calculated non-dimensional relaxation time for the conditions of Brown's experiments and determined it to be in range 10^{-4}-10^{-3}. Approximately the same range applies to the colloidal particles used in the present work. Based on Epstein's classification, Sinclair argued for diffusion dominating mechanism of the colloid transport.

Shams at al. [16] employed Direct Numerical simulations to study in detail the role of the boundary layer structure in the particle deposition process. As a result the value of the lower boundary of the inertia dominating region was adjusted to $\tau \approx 10^{-2}$ and shown to depend on the shear velocity value. They found the particle transport rate in the diffusion region to increase with decrease in shear velocity. Interestingly, that the deposition velocity they calculated has V-shape variation in the streamwise direction. This may correspond to the "ripples/fences" experimentally observed on the silica scale surface [16].

1.3 SILICA ATTACHMENT TO SURFACE

The features of the chemical process taking place at the scaling surface may provide yet other explanations to the present discrepancies in the understanding of the silica scale formation.
As for any heterogenic reaction rate of the silica scale formation is determined on one hand by the rate of silica transport to the surface, and by actual surface chemical kinetics on the other [17].

If reaction of silica attachment to the surface is instantaneous then the rate of scale growth is determined by the rate of its transport from the bulk to the surface. Whereas, if the rate constant of the surface reaction is lower than the transport rate, it determines the rate of deposition. Under such conditions the deposition process is considered to be in the kinetic region and doesn't depend on the diffusion rate at all [17].

In the kinetics of particle attachment, instead of rate constant, the term 'sticking probability' is widely used [18, 19].When multiplied by the particle transport rate to the surface it gives total reaction rate. In a study of aerosol deposition it was found to be much less than unity [19].

When geothermal brine, with both dissolved and colloidal silica in it, comes into contact with a metallic surface, first a relatively quick surface precoating with a monolayer of chemisorbed silica occurs [3]. The silicic acid molecules from solution form bonds with ionized hydroxyl groups on surface metal atoms. Once the surface is covered and sorption-desorption reactions on the surface reach equilibrium, further growth of the scale by monomeric deposition is limited by slow rearrangement of chemisorbed silica into the amorphous form, just as in the last stage of colloidal silica formation process described above [2].

The observed effect of faster scale build up by the colloidal silica if compared to the monomeric [9] is due to the following. First, presence of the ionized hydroxyl groups on the particle surface in addition to those on the wall increases chances of its attachment [2]. Second, particle attachment to the wall provides much more effective use (in terms of the scale growth) for each formed chemical bond. Since, for every surface silica atom there are ~10^3 bulk atoms which constitute the particle [1] and as only a small part of the particle surface actually attaches to the wall then for every Si-O-Si bond formed between particle and wall surface the scale growth is approx 10^4 higher than that for the monomeric silica (sorption).

Although for colloidal silica particle to come close enough to the wall for bond formation it first must overcome the electrostatic potential barrier. As mentioned before, this barrier makes colloidal systems stable towards aggregation. Due to the surface charge colloidal particles experience long-range electrostatic forces described by the DLVO theory. Once the wall has acquired a layer of amorphous silica, its charge is similar to that of the particles, and particle-wall forces are repulsive. If the particle comes into close proximity with the wall, then short-range attractive forces (London-Van der Waals) dominate, and the particle binds to the wall.

Hydrodynamic effects were found to influence stability of colloidal systems [6]. Velocity gradients and turbulent pulsations in the suspending flow force colloids to move with greater relative velocities than in the stagnant sol. This in turn increases probability of particle coagulation as a result of particle collisions. The same must be true in case of particle-wall collisions – overall flowing silica sol can be stable and still particles will aggregate to the surface due to the greater kinetic energy of their relative motion. This particular feature allows study scale formation by using stable silica aquasols.

Following [20], the total colloidal potential between the particles with radius a and the wall surface is thought to be composed of the Lifshitz-van der Waals interaction ϕ_{LW} and the electrostatic double layer potential ϕ_{EDL} as described by DLVO theory. These potentials are defined as

$$\phi_{LW} = \frac{-A}{6H}, \quad H << 1$$

$$\phi_{EDL} = \pi\varepsilon\varepsilon_0 a(\zeta_1^2 + \zeta_2^2)\left[\frac{2\zeta_1\zeta_2}{\zeta_1^2 + \zeta_2^2}\ln\left(\frac{1+\exp^{-\pi H}}{1-\exp^{-\pi H}}\right) + \ln\left(1-\exp^{-2\pi H}\right)\right]$$

where A is the Hamaker constant for interactions of the particles in the suspending medium with the wall planar surface, H is the dimensionless separation distance between the particles and the wall, ζ_1 and ζ_2 are the electrical potential (i.e., the zeta potential at shear plane) of the particle and wall, ε is the relative permittivity or dielectric constant of the medium and ε_0 is the permittivity under vacuum, $\tau = \kappa a$ is the dimensionless Debye-Huckel reciprocal length, and κ is the Debye-Huckel reciprocal length defined by

$$\kappa = \sqrt{\frac{2e^2 n_\infty z^2}{\varepsilon kT}}$$

where e is the electron charge, z is the valence, and $n_\infty = 1000 N_A C_s$ is the bulk number density of ions (ion number concentration), N_A is Avogadro's number, and C_s is the electrolyte molar concentration (ionic strength of the solution in Molar).

2 STUDY OF DEPOSITION UNDER CONTROLLED CONDITIONS

2.1 Numerical Study

The current study involves both numerical and experimental studies. For the former, a numerical model of particle deposition from a laminar, isothermal suspension onto a parallel plate channel is considered. The case of turbulent flow, although more representative of the actual problem occuring at the power plant, is more complicated both theoretically and numerically. This work can therefore be viewed as a preliminary study to a more complicated, holistic research and development that will be undertaken in the near future in this series of research projects.

For this numerical study, the effects of the various flow and physicochemical parameters on the rate of deposition were investigated. The results obtained were based on the use of a particular model by Sjollema and Busscher [20] which has been shown to provide good approximations to the experimental results of the deposition rate for some physicochemical conditions. For details of the model including the parameter values, please refer to Reference [20]. Numerical results (in terms of dimensionless initial deposition rate Sh_0) are presented to demonstrate the effect of the following parameters on the rate of deposition of the particles (i.e., parametric study): (1) the flow velocity (proportional to flow rate) (2) temperature of the carrying fluid, (3) the ionic strength of the solution, and (4) the particle size. From such a study, deeper understanding of the functional relationship between the various flow and physicochemical parameters involved in the particle deposition problem can be gained, and consequently, insight into mitigating the problem can be obtained.

2.2 Experimental Study

To study colloidal deposition under controlled hydrodynamic and chemical conditions a flow rig was constructed. The synthetic silica sol circulates thru it in a loop with a centrifugal pump controlling flow rate and flow conditioner providing uniform velocity profile at the inlet to a test section. To localise scaling to the mild steel pipe test section all other parts of the rig are made of stainless steel.

In the current design the range of the following operating conditions can be achieved on the rig:

- Reynolds number from 750 to 15000
- Temperature 20-100 °C
- Pressure 1 atm
- Dissolved oxygen concentration 0.5 mg/l

The Coriolis flow meter, pressure transducer and set of thermocouples were set up to control these parameters. The Reynolds (Re) number can be regulated both by changing flow rate and test section inner diameter (NB) thus it is also possible to set different developed velocity profile structure in the test section for the same Re.

The synthetic silica aquasol used in deposition experiments was prepared from sodium metasilicate solution by the hydrolysis method. The sol composition was roughly 99%wt water, 1500 ppm colloidal silica, 100-100 ppm silicic acid, 650 ppm sodium. By controlling the pH of the solution in range from 7 to 9 stable particles 10 to 100 nm in diameter can be grown.

3. RESULTS

3.1 Numerical

Due to the lack of comprehensive data and parameter values for the deposition of silica particles required to investigate the effects of the above parameters on the rate of deposition, the particle types employed in [20] are considered, which are polystyrene lattices with different surface charge densities: (1) type UV-82, with diameter of 736 nm, and (2) UV-148, with a diameter of 820 nm, both of which having a material density (ρ_p) of $1.05\times103 kg/m^3$. These latex particles were suspended in potassium phosphate buffers at pH of 7.0 with ionic strengths ranging from 10 to 100 mM at ambient temperature, flowing with

Exp #	Flow rate, L/min	Temp., °C	Re	Duration, days	Silica content, ppm (colloidal/monomeric)	Avg. Particle size, nm	pH
1	6.6	25	11758	14	1578/118	18	
2	6.6	25	11758	14	1578/118	14	8.8
3	6.6	25	11758	21	1578/118	17	8.5
4	31.2	34	66699	28	1555/141	21	8.9
5	31.2	34	66699	14	1555/141	28	8.1
6	6.6	45	17637	16	1524/172	27	8.3
7	31.2	45	83374	15	1524/172	27	8.3
8	6.6	45	17637	17	~0/185	-	8.4
9A	6.6	25	11758	21	1578/118	80	8.7
9B	6.6	25	11758	21	1578/118	80	8.7
10	31.2	34	66699	10	1578/118	80	8.5
11	31.2	34	66699	14	1578/118	65	8.8

Table 1: Conditions for experiments

two different flow rates: 0.15ml/s (Re = 4.0) and 0.04ml/s (Re = 1.1), which represent laminar conditions.

3.1.1 Flow Velocity

We first look at the effect of the flow velocity. For this purpose, the particle type UV-82 with four colloidal suspensions of different flow rates: 0.004, 0.04, 0.4 and 4 ml/s were considered. For each case, the ionic strength of the solution is C_s = 100mM while the temperature is chosen as T = 25°C. Figure 1 shows the dimensionless initial deposition rate (Sh_0) as a function of dimensionless length in a log-log plot. Note that the straight lines in such log-log plots indicate a power law behaviour where the slope of the lines is the exponent of the power law α. This figure shows that the deposition rate increases as the flow velocity increases. When the flow velocity increases, the problem Peclet number (the ratio of convective flux to diffusive flux) also increases, hence the higher rate of deposition.

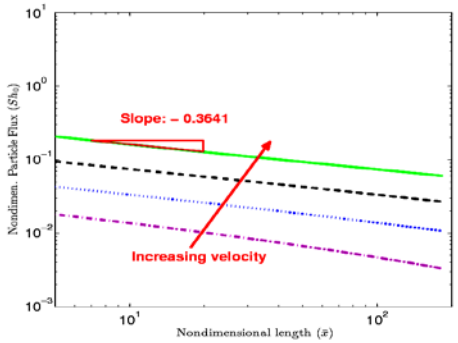

Figure 1: Parametric study - velocity

3.1.2 Temperature

Figure 2 shows the plots of Sh_0 as a function of dimensionless particles UV-82 with four colloidal suspensions of different flow temperatures: T = 25°C, 50°C, 70°C, 100°C. For each case, the ionic strength of the solution is chosen as C_s = 100mM while the flow rate is 0.04ml/s. This figure indicates, for both particle types, that the deposition rate reduces as the temperature increases. As the flow temperature increases, the problem Peclet number and the attractive ϕ_{LW} potential reduces. Hence, the deposition rate reduces.

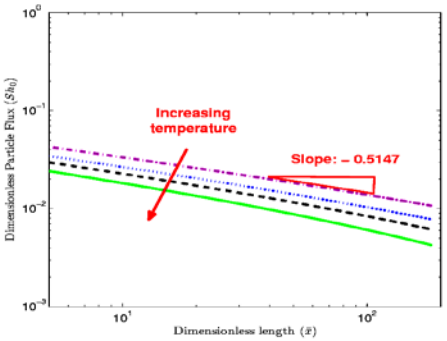

Figure 2: Parametric study - temperature

3.1.3 Ionic Strength

To investigate the effect of ionic strength on the rate of deposition, four colloidal suspensions of different ionic strength: C_s = 10, 20, 70, and 100 mM were considered. For each case, the flow rate was chosen as 0.04ml/s while the temperature was T = 25°C. The numerical results obtained show that the resulting Sh_0 for C_s = 70mM is the same as those for C_s = 100mM, while for C_s = 10mM and 20mM, Sh_0 = 0 (for both particle sizes). From these results, it can be seen that in general the rate of initial deposition increases as the value of the ionic strength increases. As ionic strength increases, the Debye-Huckel length (thickness of ϕ_{EDL}, i.e., length at which ϕ_{EDL} plays role) and the magnitude of ϕ_{EDL} decreases. Hence, deposition rate increases.

3.1.4 Particle Size

The particle size has effect in both the flow conditions and physicochemical characteristics. In a nutshell, particles with larger size will have higher rate of deposition, for the same value of flow velocity, temperature and solution ionic strength. For completeness, we show in Figure 3 comparison of the rate of deposition between the two particle types used in this study, i.e., UV-82 and UV-148, both of which with flow rate of 0.15ml/s, ionic strength Cs of 70mM, and temperature T of 50°C. As particle size increases, the diffusion coefficient decreases, and therefore the Peclet number increases and the Debye-Huckel length decreases, resulting in higher deposition rate.

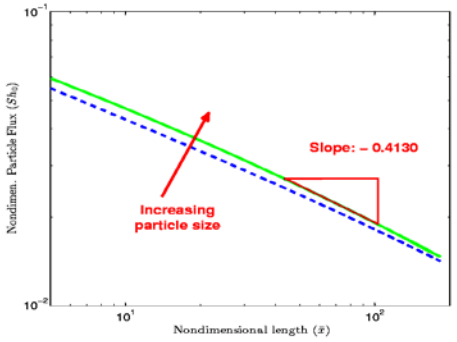

Figure 3: Parametric study – particle size

3.2 Experimental

Twelve scaling experiments were conducted in the first year of operation of the rig. Preliminary results on the scale growth rate, morphology and composition were obtained.

In each experiment test section was 150mm long mild steel pipe of 15mm ID. The range of the hydrodynamic conditions tested is shown in Table 1.

Two different recipes for sol production were tried, which allowed comparison between two particle size ranges: from 15 to 30 and from 65 to 80 nm. In experiment #8 a solution with only monomeric silica (no particles) was used. Each experiment lasted 2-3 weeks with occasional deviations due to operational difficulties. Over this time the particle size was stabilized by keeping the pH value over 8.

Flow rate was measured with uncertainty of ±0.1 l/min. The sol temperature was measured at two points, just after the mixing tank and after test section, and usually remained within ±4°C of the setpoint.

Preliminary experiments showed primary silica particles agglomerating on rust deposits (fig.4). Greater deposition

was observed at the inlet. After this a nitrogen blanket and oxygen scavenger were installed in the rig and the dissolved oxygen level was kept below 30% of saturation. No further rust was seen.

Welded (fire sprinkler) pipe was used in the first 8 experiments. The systematic absence of deposits in the near weld region was noted. The use of seamless pipe eliminated this feature but introduced another irregularity due to non-uniform surface properties.

The morphology and rate of scale formation was found to depend on flow rate and chemical conditions. Comparison of experiments # 3 and #4 shows that localized deposition of packed globules and porous structures may form at higher flow rates (see fig.5 and 6). More deposition was observed on the outlet end in Exp #4.

Formation of non-spherical aggregates was observed at increased temperature (see fig. 7), perhaps due to the increased solubility of silica.

Very little scaling, and no globular or any other complex structures formed in the experiment with monomeric silica deposition (compare fig.6 and7 with fig. 8).

The effect of increasing the size of the colloidal silica particles is seen in experiment # 10 (fig. 9) where the deposits appear to consist of large, overlapping agglomerations.

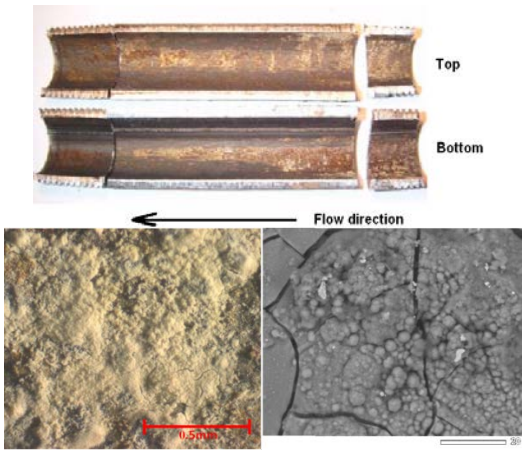

Figure 4: For Exp#2

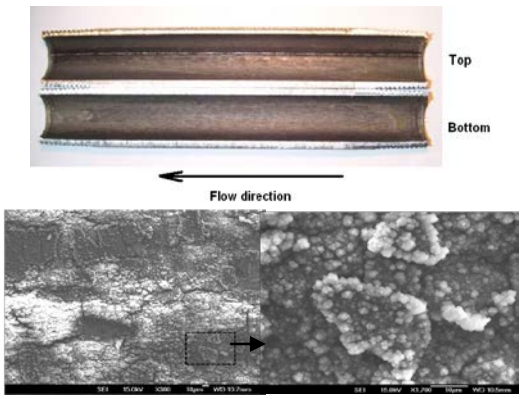

Figure 5: For Exp#3

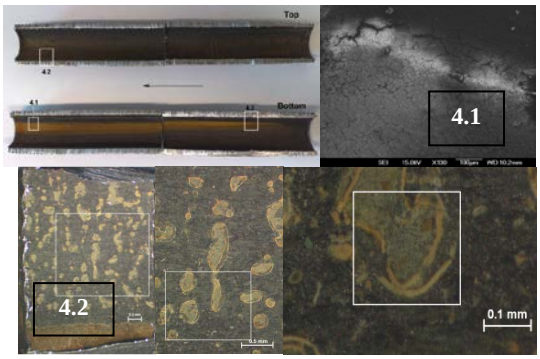

Figure 6: For Exp#4

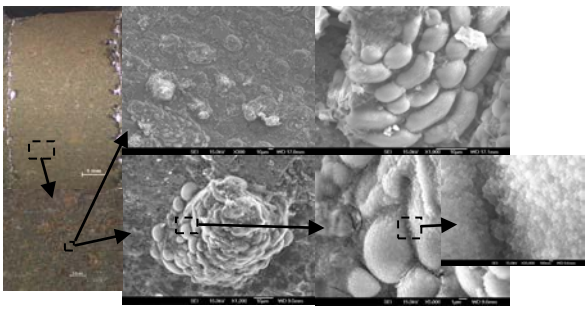

Figure 7: For Exp#7

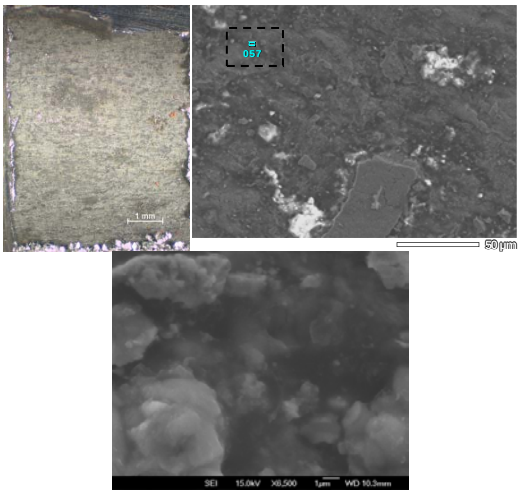

Figure 8: For Exp#8

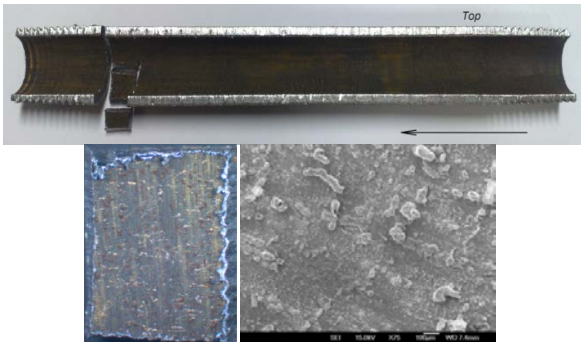

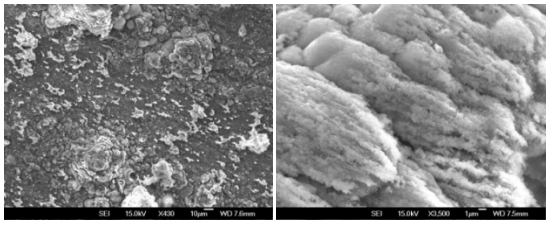

Figure 9: For Exp#10

4. DISCUSSION AND CONCLUSIONS

4.1 Numerical

Based on the results of the parametric studies discussed in Section 3.1, the rate of initial deposition of particles can be reduced if

• particle size is smaller

• flow velocity is reduced

• flow temperature is increased

• ionic strength is reduced

It is, however, important to mention that there are no temperature gradients in the current model, but such gradients exist in geothermal plant. Where temperature gradients exist, the suspension is subject to an additional contribution to the deposition of the particles due to thermophoresis. It is recommended that any future work in this study takes thermophoresis into account to obtain more reliable and representative results.

4.2 Experimental

The rate of deposition reduces with temperature (the solubility of silica increases, and Brownian diffusion away from the surface increases). The rate of deposition increases with flow rate (due to changes in the near-wall velocity structure and eddy transport, as well as due to the effects noted in the laminar flow numerical modelling, which will also exist in the turbulent flow in the rig). These trends are also seen in the numerical model.

Deposition of silica particles is observed frequently on edges and cracks in the pipe wall, and less frequently in the plains between these features. This may be explained by the local surface energy, the bridging oxygen configuration or by local hydrodynamic conditions at these edge sites.

The initial deposition is observed to occur in isolated clusters or clumps. The reasons for this are not yet clear, but may be related to local hydrodynamic effects. Immediately downstream of an irregularity on the wall, there will be a flow recirculation region with low wall shear stress. Recently arrived particles may be more likely to bind permanently with the surface in these regions. Inertial effects in these regions may increase the rate of arrival of particles . In this way, local irregularities may accumulate particles, and this local scale growth may enlarge the initial irregularity, enhancing the processes mentioned above, leading to further growth of the scale deposit locally. This may explain the “fences” and cellular structures seen in long-term scale deposition. This hypothesis will be tested in future experiments.

ACKNOWLEDGEMENTS

We wish to thank Mighty River Power for supporting this study and in particular Michael Rock, Simon Addison and Jeff Winick for technical advice.

REFERENCES

1. R. K. Iler, *The chemistry of silica: solubility, polymerization, colloid and surface properties, and biochemistry*: Wiley, 1979.

2. B. A. Fleming: *Kinetics of reaction between silicic acid and amorphous silica surfaces in NaCl solutions*, Journal of Colloid and Interface Science, vol. 110, pp. 40-64. (1986).

3. O. Weres, et al.: Kinetics of silica polymerization, Journal of Colloid and Interface Science, vol. 84, pp. 379-402. (1981).

4. R. J. *Hunter, Introduction to modern colloid science*, Oxford University Press, Oxford, 1993.

5. R. Brown: *A brief account of microscopical observations made in the months of June, July and August, 1827, on the particles contained in the pollen of plants; and on the general existence of active molecules in organic and inorganic bodies*. Phil. Mag. 4, pp. 161–173. (1828).

6. V. Levich, *Physicochemical hydrodynamics*: Prentice-Hall, Inc., 1962.

7. K.R. Applin: *The diffusion of dissolved silica in dilute aqueous solution*. Geochim. Cosmochim. Acta, 51, pp. 2147-2151. (1987).

8. K. L. Brown and M. Dunstall: *Silica scaling under controlled hydrodynamic conditions*, in World Geothermal Congress, Kyushu-Tohoku, Japan, pp. 3039-3044. (2000).

9. M. Dunstall, H. Zipfel and K. L. Brown: *The onset of silica scaling around circular cylinders*, World Geothermal Congress, Kyushu-Tohoku, Japan, pp. 3045-3050. (2000).

10. S. K. Friedlander, H. T. Johnstone: *Deposition of suspended particles from turbulent gas stream*. Industrial and Engineering Chemistry, 49, pp. 1151-1156. (1957)

11. G. A. Kallio, M. W. Reeks: *A Numerical Simulation of Particle Deposition in Turbulent Boundary Layers*. Int. J. Multiphase Flow 15, pp. 433-446. (1989).

12. S. T. Johansen: *The Deposition of Particles on Vertical Walls*. Int. J. Multiphase Flow 17, pp. 355-376, (1991).

13. P. G. Saffman: *The Lift on a Small Sphere in a Slow Shear Flow.* .J. Fluid Mech. 22, pp. 385-403. (1965).

14. N. Epstein: *Elements of particle deposition onto nonporous solid surfaces parallel to suspension flows.* Experimental Thermal and Fluid Science, vol. 14, pp. 323-334. (1997).

15. L. A. Sinclair, "Development of a Silica Scaling Test Rig," *Masters, University of Canterbury*, Christchurch, 2012.

16. M. Shams, G. Ahmadi and H. Rahimzadeh: *A sublayer model for deposition of nano- and micro-particles in turbulent flows*, Chemical Engineering Science, 55, pp. 6097-6107. (2000).

17. D. A. Frank-Kamenetskii, *Diffusion and Heat Transfer in Chemical Kinetics* (in Russian), Moscow-Leningrad: USSR Academy of Science Press (1947); ((in English): Springer-Verlag, 1955; Princeton University Press, 1969)

18. A.G. Konstandopoulos: *Particle sticking/rebound criteria at oblique impact*. Journal of Aerosol Science Volume 37, Issue 3, pp. 292–305. (2006).

19. S. G. Yiantsios, A. J. Karabelas: *Deposition of micron-sized particles on flat surfaces: Effects of hydrodynamic and physicochemical conditions on particle attachment efficiency*. Chemical Engineering Science 58, pp. 3105 – 3113. (2003)

20. J. Sjollema and H.J. Busscher: *Deposition of Polystyrene Latex Particles toward Polymethylmethacrylate in a Parallel Plate Flow Cell*. Journal of Colloid and Interface Science, 132(2), pp. 382–394. (1989).